SAND2011-0751C

2011 7th US National Combustion Meeting
Organized by the Eastern States Section of the Combustion Institute
and Hosted by the Georgia Institute of Technology, Atlanta, GA
March 20-23, 2011

Evaluation of the Combustion Rates of Lignin Residues from Cellulosic Ethanol Production

C.R. Shaddix, E. Hecht, and M. Geier

Combustion Research Facility, Sandia National Laboratories,
Livermore, California 94550, USA

Cellulosic ethanol is a promising alternative to conventional starch- and sugar-based ethanol production in terms of potential production quantities, CO_2 impact, and economic competitiveness. However, approximately 1/3 of most lignocellulosic biomass feedstocks (including all of the lignin) cannot be converted to ethanol through biochemical means and is extracted at some point in the biochemical process. In this work we have evaluated the rapid heating volatile yields and char burning rate of such lignin residue material, generated through several different biochemical processing techniques applied to corn stover and eucalyptus feedstocks. Char reactivity was deduced from optical measurements of char particle combustion temperatures in a laminar entrained flow reactor. The lignin residue chars show somewhat lower reactivity than corresponding raw biomass chars, except for the residue from dilute-acid simultaneous saccharification/fermentation (SSF), which shows substantially lower reactivity. In comparison to an existing database on coal char reactivity in an identical furnace environment, most of the residues have char combustion reactivities comparable to high-volatile bituminous coals.

1. Introduction

Dwindling supplies of conventional oil and increasing concern over greenhouse gas emissions have motivated the development of cost-effective approaches for generating renewable liquid fuels. Biomass-derived liquid fuels are promising candidates, particularly in the U.S., with its large capacity for growing biomass. Currently, farm and ethanol subsidies and a guaranteed ethanol market have fostered the production of a large corn ethanol market. However, corn-based ethanol production engenders significant CO_2 production and has limited potential to offset U.S. oil consumption. Far greater production potential and improved reductions of CO_2 are possible when converting lignocellulosic biomass (grasses, trees, crop residues, etc.) into ethanol [1,2].

Biochemical processing of lignocellulosic biomass can typically only convert 60-70% of the biomass feedstock to C_6 and C_5 sugars, for subsequent fermentation to ethanol, because of the existence of several components of the biomass, particularly lignin, protein, and extractives, that do not contain sugar polymers. This non-fermentable portion of the biomass can undergo partial water removal (for example, by centrifuging) and then be used as a fuel for thermal processing, via combustion, gasification, or pyrolysis, as suggested by Fig. 1 [3]. To realize an efficient, integrated lignocellulosic ethanol biorefinery, as suggested in Fig. 1, the relevant fuel properties of typical ethanol residuals need to be determined, such that suitable combustion, gasification, and pyrolysis reactors can be built and operated. This paper reports on our analysis of the combustion reactivity of residues produced by several promising biochemical ethanol processes. Previous studies of the thermochemical conversion of ethanol production residues have been very limited and have focused on ash behavior in boilers [4], overall performance in a pellet stove [5], overall performance in a powder burner [6], and catalytic gasification to produce H_2 [7]. The current study, in contrast, focuses on generating the fundamental conversion rate information that is important to both a phenomenological understanding of and an ability to model the behavior of these residues in different thermochemical processes.

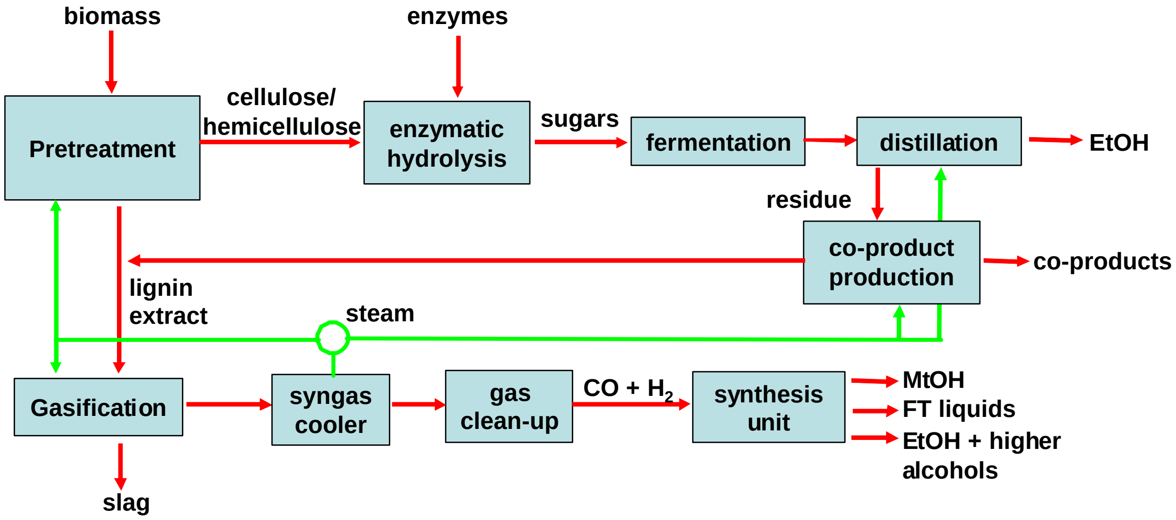

Figure 1: **Schematic illustration of a potential future design layout for a lignocellulosic ethanol biorefinery with primarily biochemical conversion and gasification of lignin residues.**

2. Lignin Residues

Lignocellulose ethanol process residues were generated from two sources: (1) from small-scale batch processing of biomass using low-cost pretreatment processes that directly separate lignin from the cellulose in the pretreatment step, and (2) from the pilot-scale dilute acid hydrolysis simultaneous saccharification and fermentation (SSF) process at the National Renewable Energy Laboratory (NREL).

The pretreatment approach known as “soaking in aqueous ammonia” (SAA) [8-11] was applied to corn stover and eucalyptus wood samples. In this process lignin is solubilized in the ammonia solution, together with a portion of the hemicellulose (linked C_5 and C_6 sugars). Subsequent drying of the solution yields a lignin residue.

The Arkenol pretreatment process [12-14], which utilizes strong sulfuric acid to hydrolyze cellulose and hemicellulose in the biomass, was applied to eucalyptus wood samples. This process can either be implemented as a single-stage hot acid soak or in two stages. Lignin residue samples from both the single-stage and dual-stage processing were collected for this study.

The most widely used lignocellulose pretreatment approach is undoubtedly dilute sulfuric acid pretreatment, which does not effectively hydrolyze the carbohydrates and therefore requires subsequent enzymatic hydrolysis, after neutralization and detoxification, to complete the hydrolysis of the polysaccharides (i.e. to complete "saccharification"). NREL has a pilot-plant configuration that has been investigating and optimizing dilute sulfuric acid pretreatment of corn stover followed by simultaneous saccharification and fermentation (SSF), a cost-reducing intensification of the process path. After distillation of the ethanol, the lignin-containing process dregs are removed. For this project, NREL researchers provided us with a sample of the lignin residue from their SSF process, when processing corn stover.

Ultimate, proximate, ash, and heating value analyses were performed on the lignin residues, as well as on the raw feedstocks from which they were generated. Some of the more important results are shown in Figs. 2 and 3. The corn stover SSF residue has a substantially higher ash content (which is dominated by silica) than any of the other samples, and the eucalyptus residues have higher heating values than either the raw biomass or the corn stover residues.

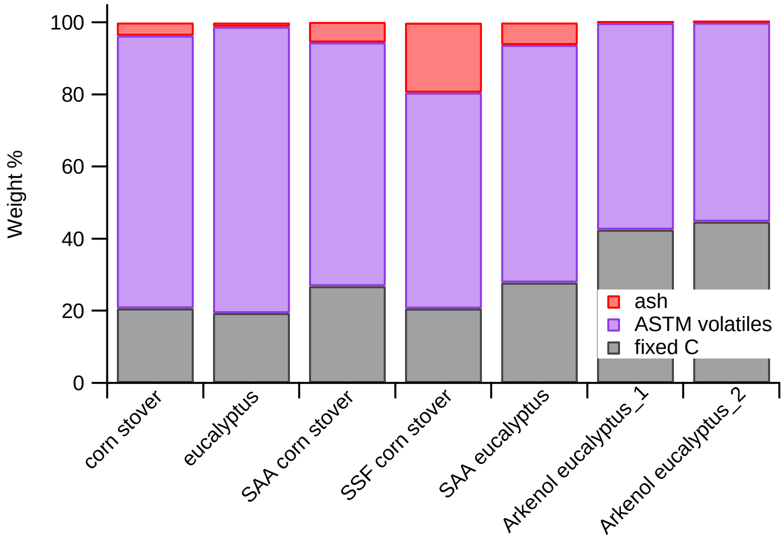

Figure 2: Summary of proximate analysis of raw feedstocks and associated lignin residues.

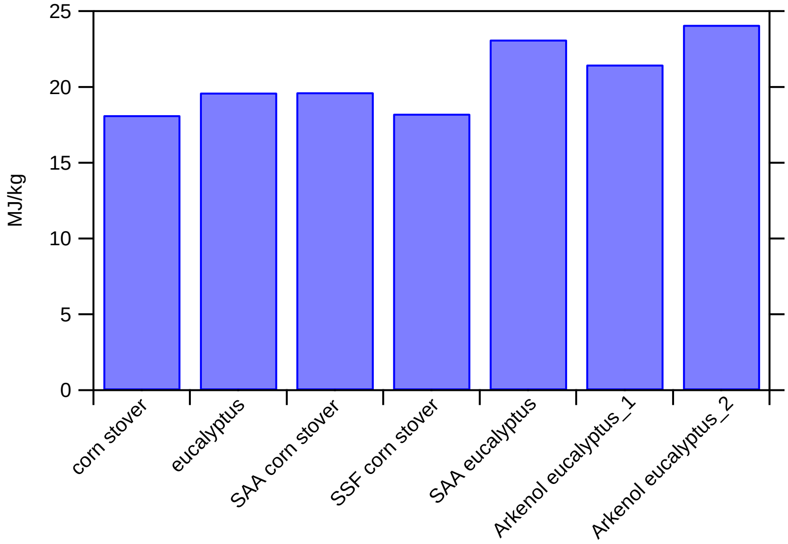

Figure 3: Heating values, on a dry basis, of raw feedstocks and associated lignin residues.

3. Experimental Approach

Samples of the raw biomass and the associated lignin residues were dried at low temperatures and then milled in a Wiley knife mill outfitted with a custom-sized tail screen. The milled particles were then sieved using a Retsch vibratory sieve shaker.

Two different high-temperature flow reactors were utilized to characterize the behavior of the lignin residues, as shown in Fig. 4. The first reactor is an electrically heated, downflow, enclosed reactor known as the Pressure-Capable Entrained Flow Reactor (PCEFR). The PCEFR exhaust has a water-cooled gas-diluent quench followed by a cyclone particle collector. This reactor was used in this study to determine the high heating rate volatiles yield of the residues by feeding finely milled particles into a preheated nitrogen flow at 1473 K. The nitrogen flow rate and particle sampling position were set to expose the residue particles to the hot gas flow for 250 ms, which should be sufficient to fully devolatilize the feed particles.

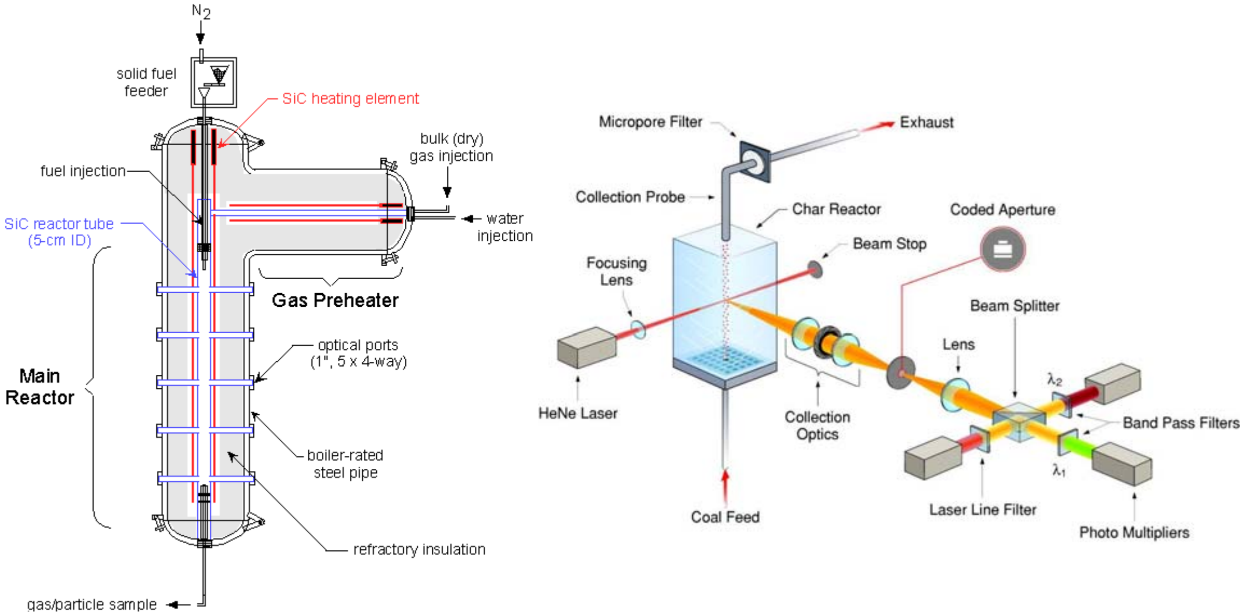

Figure 4: Schematic illustrations of Sandia's Pressure-Capable Entrained Flow Reactor (left) and combustion-driven optical entrained flow reactor (right).

The PCEFR also proved to be beneficial in producing pre-generated char particles for feeding into a second reactor, a combustion-driven optical entrained flow reactor that has been widely used to characterize pulverized coal particle reactivities and deduce char combustion kinetics [15,16]. The optical entrained flow reactor utilizes single particle imaging through a coded aperture to simultaneously measure the size, velocity, and temperature of individual reacting char particles as they are convected in the flow. For this study, a common gas temperature of 1650 K and a range of oxygen concentrations between 12 vol-% and 36 vol-% was utilized, to allow direct comparison of the biomass char burning rates with previously collected data for a wide range of coal rank [17].

Initial experiments aimed at characterizing the combustion reactivity of the residues in the optical entrained flow reactor were largely unsuccessful, because of difficulties feeding the residues at a uniform rate, the extensive amount of devolatilization (reducing the particle size and moving the particles off of the reactor centerline where the optical diagnostic probe volume is located), and the limited available quantity of the residues. By devolatilizing the residue particles first in the enclosed reactor, improved optical data during char particle combustion could be obtained. Furthermore, by devolatilizing the residue particles first in the PCEFR, we remove the possibility of char combustion effects from variations in the devolatilization process in the optical entrained flow reactor when raw particles are fed into environments with different oxygen concentrations. For the lignin residues (and for their associated raw biomass feedstock), a particle size range of 75-180 μm was fed into the PCEFR and the collected char particles were re-sieved to 75-106 μm for feeding into the optical EFR.

4. Results

Proximate analysis of the char particles collected from the PCEFR allowed the determination of the high heating rate volatiles yield of the raw eucalyptus, as well as that of the Arkenol process lignin residues generated from eucalyptus. Based on past experience with similarly sized coal particles introduced into similar thermal environments, we estimate the initial particle heating rate of the biomass particles to be 10^4-10^5 K/s. The volatiles yields, based on the traditional ash tracer analysis technique, are shown in Fig. 5, together with the ASTM volatiles content that was measured from the original proximate analysis of the feed material. As shown in Fig. 5, the high heating rate volatiles loss of the particles far exceeds the ASTM volatiles content (determined under low heating conditions), especially for the lignin residues. In fact, all three biomass materials analyzed have a high heating rate volatiles loss of over 90 wt-%, in agreement with the limited data available in the literature (for raw biomass only) [18]. This very high volatiles yield promises good overall reactivity of the lignin residues (at least when dry) when they are finely milled and introduced into either combustion or high-temperature entrained flow gasification environments. For lower temperature bed-based processes with larger fuel particles, the volatiles loss will probably approximate the ASTM level, leaving substantially more char to convert in the relatively slow char oxidation or gasification processes. The results shown in Fig. 5 suggest that the lignin residues are likely to produce fewer volatiles and leave more char to be gasified in these environments.

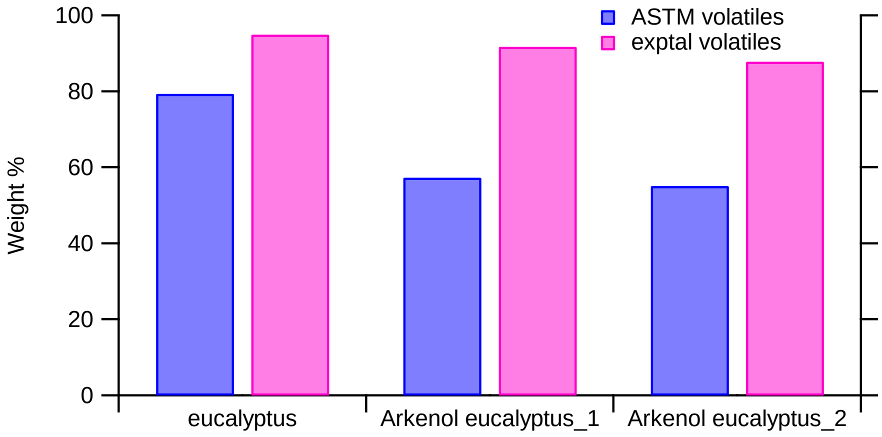

Figure 5: Comparison of ASTM volatiles content and measured high heating rate volatiles yield.

Char particle combustion temperatures in the optical entrained flow reactor showed the typical initial rise in char temperatures with height in the flow reactor, followed by a fall as some of the particles approached final burnout. To characterize the relative reactivity of the different fuels investigated, it is useful to first compute the mean char particle temperature profile in the reactor and then to compare the maximum mean temperatures reached by the different fuels, as a function of reactor conditions. Such a comparison is shown in Fig. 6. This comparison of char particle temperatures does not map directly into relative reactivity because of the potential issue of differences in char particle sizes and shapes, particularly for the biomass fuels in comparison to the coal chars. The optical particle sizing gave approximately equal mean particle sizes for all of these fuels, but biomass particles are well-known to often exhibit strong variations in aspect ratio (on account of fiber directions), which could distort the optical signals. Ignoring this complication, for the time being, the results shown in Fig. 6 suggest that raw biomass produces more reactive chars than any of the lignin residues. Among the residues, the SAA and Arkenol approaches generate material that has similar combustion reactivity, whereas the high ash SSF residue is substantially less reactive. In comparison to coal chars, the raw biomass chars have similar reactivity to low-rank coals (subbituminous to high volatile bituminous), while the SAA and Arkenol chars are as reactive as medium-rank coals (low volatile to high volatile bituminous), and the SSF residue is as unreactive as high-rank coals (e.g. anthracite).

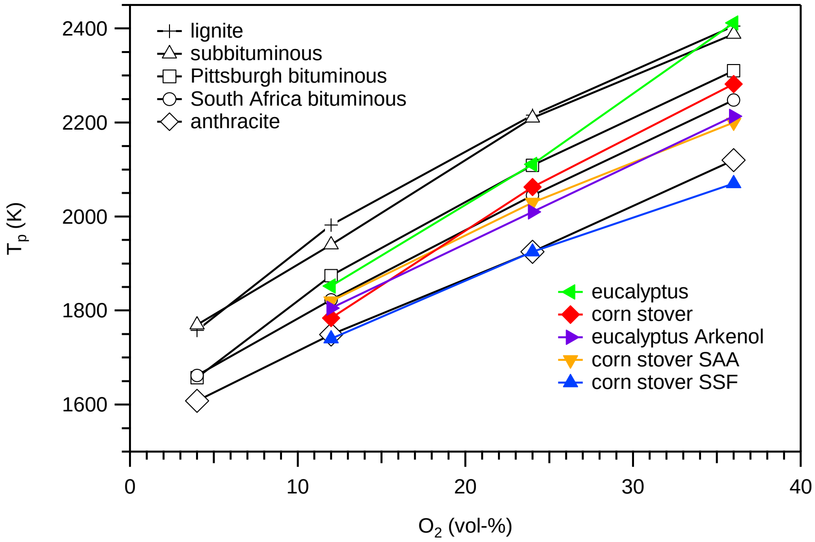

Figure 6: Comparison of maximum mean char particle temperatures reached for each of the fuels listed, as a function of oxygen content in a furnace flow at 1650 K. Results for different types of coal are indicated by black symbols and lines and the biomass results are given in color.

5. Conclusions

The high temperature, high heating rate volatiles loss was measured for corn stover and eucalyptus and for lignin residues from these feedstocks generated through different lignocellulosic ethanol processes. In addition, char combustion temperatures were measured from these fuels in an optical entrained flow reactor. The high heating rate volatiles loss was greater than 90% for all investigated biomass fuels and was substantially higher than the low heating rate ASTM volatiles loss, especially for the lignin residues. The apparent char combustion reactivities ranged from high values for the raw biomass to quite low value for the SSF residue. The other residues showed intermediate levels of char combustion reactivity, probably reflecting the large silica ash content of this material.

Acknowledgments

Adam Bratis of the National Renewable Energy Laboratory graciously provided the SSF residue. Dean Dibble and George Buffleben of Sandia National Laboratories provided the SAA and Arkenol pretreatment process residues. This work was supported by the Laboratory Directed Research and Development program at Sandia National Laboratories. Sandia is a multiprogram laboratory operated by Sandia Corporation, a Lockheed Martin Company, for the United States Department of Energy’s National Nuclear Security Administration under Contract DE-AC04-94AL85000.

References

[1] C.N. Hamelinck, G. van Hooijdonk, A.P.C. Faaij, *Biomass Bioenergy* 28 (2005) 384–410.
[2] D.D. Hsu, D. Inman, G.A. Heath, E.J. Wolfrum, M.K. Mann, A. Aden, *Environ. Sci. Technol.* 44 (2010) 5289–5297.
[3] C.R. Shaddix, E. Hecht, K.-Y. Teh, G. Buffleben, D. Dibble, A. Lutz, *Development of Efficient, Integrated Cellulosic Biorefineries: LDRD Final Report*, Sandia Internal Report, SAND2010-7141, Oct. 2010.
[4] S.L. Blunk, B.M. Jenkins, *Combustion Properties of Lignin Residue from Lignocellulose Fermentation*, UC Davis Report to National Renewable Energy Laboratory, April 2000.
[5] M. Öhman, C. Boman, *Energy Fuels* 20 (2006) 1298–1304.
[6] G. Eriksson, B. Kjellström, B. Lundqvist, S. Paulrud, *Fuel* 83 (2004) 1635–1641.
[7] W.-Z. Li, Y.-J. Yan, T.-C. Li, Z-W. Ren, M. Huang, J. Wang, M.-Q. Chen, Z.-C. Tan, *Energy Fuels* 22 (2008) 1233–1238.
[8] H.H. Yoon, Z.W. Wu, Y.Y. Lee, *Appl. Biochem. Biotech.* 51/52 (1995) 5-19.
[9] T.H. Kim, J.S. Kim, C. Sunwoo, Y.Y. Lee, *Biores. Technol.* 90 (2003) 39-47.
[10] T.H. Kim, Y.Y. Lee, *Biores. Technol.* 121-124 (2005) 1119-1132.
[11] T.H. Kim, Y.Y. Lee, *Biores. Technol.* 136-140 (2007) 81-92.
[12] W.A. Farone, J.E. Cuzens, U.S. patent no. 5,620,877 (1997).
[13] W.A. Farone, J.E. Cuzens, U.S. patent no. 5,726,046 (1998).
[14] J.C. Cuzens, J.R. Miller, *Renewable Energy* 10 (1997) 285-290.
[15] D.A. Tichenor, S. Niksa, K.R. Hencken, R.E. Mitchell, *Proc. Comb. Inst.* 20 (1984) 1213-1221.
[16] J.J. Murphy, C.R. Shaddix, *Combust. Flame* 144 (2006) 710-729.
[17] C.R. Shaddix, E.S. Hecht, S. Jimenez, S.M. Lee, *Evaluation of rank effects and gas temperature on coal char burning rates during oxy-fuel combustion*, Proc. 34th International Technical Conference on Coal Utilization and Fuel Systems, Clearwater FL, May 31 – June 4, 2009.
[18] A. Bharadwaj, L.L. Baxter, A.L. Robinson, *Energy Fuels* 18 (2004) 1021-1031.